OPERATIONAL ENERGY AND POWER RESERVES FOR HYBRID-ELECTRIC AND ELECTRIC AIRCRAFT

I. Geiß, A. Strohmayer, University of Stuttgart,
Institute of Aircraft Design, Pfaffenwaldring 31, 70569 Stuttgart, Germany

Abstract

Power and energy reserves in hybrid-electric and electric aircraft propulsion systems are required to counter propulsion component failures and to cope with disorder in flight operations. In the first section of the paper, a failure of a battery pack or a combustion engine during take-off is considered and an equivalent level of safety to conventional aircraft is suggested. In the next section, a required energy reserve for a propulsion component failure during cruise flight is evaluated. Therefore, a range to reach a suitable airport for an emergency landing is determined for Europe and the USA by calculating the distance to the nearest diversion airport for a mesh of possible aircraft positions. The median, the 95th percentile and the 99th percentile of this diversion range is then determined by a cumulative frequency analysis – the investigation is carried out for different runway lengths which represent different aircraft classes. Furthermore, safety margins are discussed which are required for flight operation. The same methodology is then applied to determine the operational flight reserve which is required to reach a suitable alternate airport from a destination airport and the results are discussed.

1. NOMENCLATURE

Symbols

C_{Earth}	Circumference of Earth
$F(x)$	Cumulative frequency
$M(x)$	Number of data points below the threshold x
n	Number of data points
n_{Bat}	Number of battery packs
n_{ICE}	Number of combustion engines
$P_{Bat,max}$	Maximum rated power of battery system
$P_{Bat,TO}$	Power of battery system during take-off
$P_{ICE,max}$	Maximum rated power of combustion engines
R	Length of great circle
S_{TO}	Battery power split during take-off

Greek symbols

ζ	Angle of great circle
λ	Longitude
ϕ	Latitude

Abbreviations

Bat	Battery pack
CS	Certification specification
ICE	Internal combustion engine
IFR	Instrument flight rules
NASA	National Aeronautics and Space Administration
OEI	One engine inoperative
VFR	Visual flight rules

2. INTRODUCTION

Current research aims to exploit the characteristics of electric motors. These offer e.g. less variation of the efficiency on partial power settings than combustion engines and no dependency between rated power and maximum efficiency. Electric motors are more compact and lighter than piston engines applied in aviation [1]. As a result, electric motors are integrated in unconventional positions of the aircraft e.g. wing tip propellers are expected to decrease induced drag or gain propulsive efficiency [2]. Motors distributed along the wingspan can be utilized as a high-lift system to size a wing for an efficient cruise flight [3]. In some applications the integration in the vertical tail can increase the integration efficiency of a propeller [4]. To overcome the low specific energy of current battery cells, hybrid-electric aircraft concepts are investigated to leverage the advantage of distributed electric propulsion and combine it with the superior specific energy of fuel.

In conventional single-engine aircraft an engine failure is associated with a complete loss of propulsive power. In a series hybrid-electric aircraft several additional components are placed between the combustion engine and the propeller as shown in FIG. 1. All these components are associated with individual failure rates, which increase the likelihood of the failure mode. Hence, one option to reach an equivalent level of safety for a series hybrid-electric aircraft in this class could be that the battery system provides additional electrical power in case of a combustion engine failure. Further, if a combustion engine failure occurs during cruise flight, the battery system would need to provide energy for a flight to reach a suitable diversion airport. Several projects are currently realized with a serial hybrid-electric propulsion system and one combustion engine: e.g. Diamond DA40 Hybrid, Traveller Hybrid and e-Genius Hybrid [5].

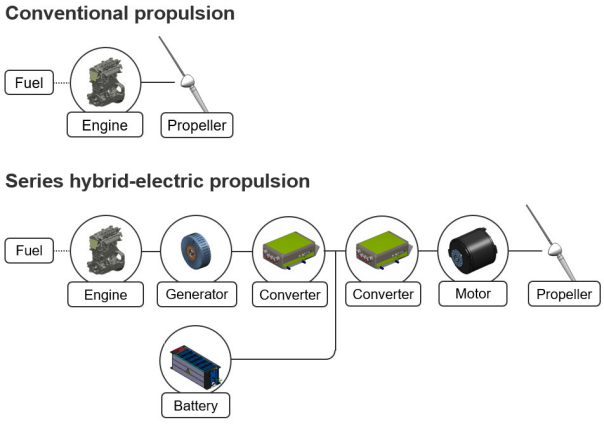

FIG. 1: Components of conventional and series hybrid-electric propulsion systems

In conventional multi-engine aircraft, a “one-engine-inoperative” (OEI) scenario is associated with a partial loss of propulsive power. However, there is no loss of energy available on-board for propulsion. This is because the fuel tank, as the energy storage, stays functional after such event. Contrary, due to the different nature of several hybrid-electric propulsion systems, an OEI-scenario may be associated with a loss of power and furthermore only a fraction of the energy stored in the fuel tank might be usable for the remaining flight. One example is the aircraft concept “PEGASUS”, which is investigated by NASA [6], where a combination of a gas turbine and an electric motor is integrated at the wing tip and further electric motors are installed on wing inboard positions and at the aft of the fuselage. The gas turbines are intended to provide in cruise flight the required thrust and thereby lowering the induced drag while achieving an increased range by the use of fuel. The propellers of the other electric motors, which are installed at the wing, are folded in cruise and do not provide thrust. If one gas turbine fails, the electric motors need to counter the yawing moment which is induced by the remaining gas turbine and contribute thrust until an emergency landing has been carried out.

The additional required allowances in the propulsion system are associated with a mass growth, which increases the energy consumption of the aircraft. Consequently, the aircraft designer shall assume reserves, which are sufficient for a safe operation but ensure a minimal mass growth. The identification of the required reserves shall be the objective of this paper. In the first section, power reserves are investigated. In the second section, energy reserves are identified, which might be required for hybrid-electric aircraft. In the third section, distances to alternate airports are investigated, with the aim to determine suitable values for hybrid-electric and battery-electric aircraft.

3. POWER RESERVES DURING TAKE-OFF

Section EHPS.80 of the draft version of the special condition for electric and hybrid propulsion systems of the EASA [7] requires a safety assessment of the propulsion system. For a series hybrid-electric aircraft, subject to CS-23, which is propelled by a single electric motor as shown in FIG. 2 different power reserves for the hybrid-electric propulsion system are plausible. In case of a failure of the combustion engine or a failure in the battery system during take-off, the following options regarding the power loss are possible:

- No compensation of the power loss (similar to current single-engine general aviation aircraft)
- Partial compensation of the power loss to achieve a positive climb gradient according to CS 23.2120
- Full compensation of the power loss

FIG. 2: Series hybrid-electric aircraft in CS-23 class: electric motor installed in vertical tail, combustion engine with generator integrated in the nose cone, battery system installed behind passengers [8]

No compensation of the power loss is not considered, as the feasibility for certification is questionable because more components in a series hybrid-electric propulsion system contribute to the failure rate. A partial compensation of the power loss might require a multi-engine pilot training, as a take-off with a climb angle of merely 1 % requires detailed flight planning and pilot skills. This would handicap the introduction of series hybrid aircraft as less pilots would be able to fly these aircraft. As a result, full power compensation shall be regarded as the equivalent level of safety. Consequently, the power loss of a combustion engine during take-off needs to be compensated by battery power. A battery system consists of several battery packs, which are all connected to the same bus bar. In case of a failure of an individual battery pack (e.g. due to a failure of a battery cell) it can be disconnected from the bus bar via a relay. The housing of a battery pack is required to contain a fire and to prevent a pack to pack propagation of it. This can be realized e.g. with an appropriate firewall and separated installation spaces for the battery packs. The excess power of the battery system needed to compensate a failure of a combustion engine during take-off, can be used to compensate a failure of a battery pack as well as shown in FIG. 3. As a result, no additional battery mass is needed. However, a specific minimum number of battery packs is necessary.

This minimum number of battery packs n_{Bat} can be deduced by requiring that the power loss due to a combustion engine failure is equal to the power loss associated with a failure of a battery pack as described with the following equation, where $P_{ICE,max}$ denotes the total combustion engine power, n_{ICE} the number of combustion engines and $P_{Bat,max}$ the total battery power available.

$$1/n_{ICE} \cdot P_{ICE,max} = 1/n_{Bat} \cdot P_{Bat,max} \quad (1)$$

$$\text{with } P_{Bat,max} = \frac{n_{Bat}}{n_{Bat}-1} \cdot P_{Bat,TO} \quad (2)$$

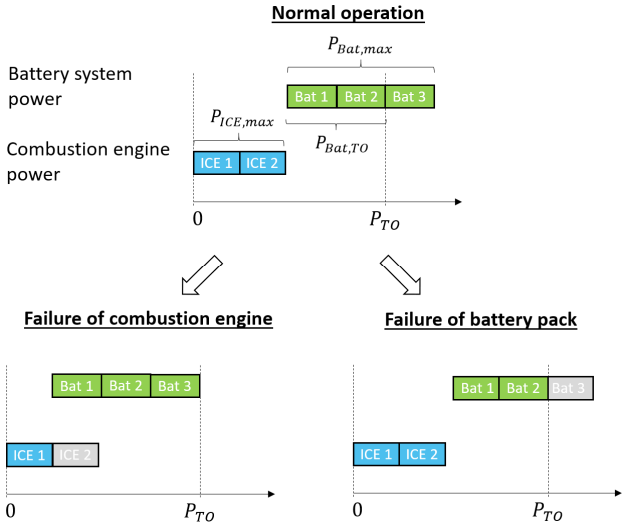

FIG. 3: Sizing of a hybrid-electric propulsion system, which can compensate the power loss resulting from a combustion engine or a battery pack failure

During the aircraft's take-off the power P_{TO} is the sum of total combustion engine power $P_{ICE,max}$ and power provided by the battery system $P_{Bat,TO}$.

$$P_{TO} = P_{ICE,max} + P_{Bat,TO} \tag{3}$$

The power split during take-off S_{TO} as defined in [9] and [10] is given in equation 4. It is a design parameter for hybrid-electric aircraft and describes which fraction of the required shaft power during take-off P_{TO} is covered by the power of the battery system $P_{Bat,TO}$.

$$S_{TO} = \frac{P_{Bat,TO}}{P_{TO}} \tag{4}$$

The power split S_{TO} is introduced into equation 3 and therein the total combustion engine power $P_{ICE,max}$ is substituted. Consequently, a relation between the number of combustion engines n_{ICE}, power split S_{TO} and required number of battery packs is deduced as shown in the following equation.

$$n_{Bat} \geq \frac{(n_{ICE} - 1) \cdot S_{TO} + 1}{1 - S_{TO}} \tag{5}$$

It is shown in TAB. 1 that the required segmentation of the battery system n_{Bat} stays within a feasible range. As only integer values are acceptable for the number of battery packs n_{Bat}, the resulting values from the equation are brought up to a round figure. Evaluating the function for $S_{TO} = 1$, which equals to a take-off carried out purely by battery power, results in a non-feasible result for the number of battery packs. This is a theoretical result, which arises from the assumption that the loss of power due a failed combustion engine shall be equal to the power loss due to a failure of a battery pack.

S_{TO}	n_{Bat} for $n_{ICE} = 1$	n_{Bat} for $n_{ICE} = 2$
0.0	1	1
0.2	2	2
0.4	2	3
0.6	3	4
0.8	5	9

TAB. 1: Minimum number of segmentations of the battery system n_{Bat} in order to compensate a battery pack failure during take-off

After a failure of a combustion engine during take-off, the battery system is required to provide power as described before. Furthermore, sufficient battery capacity is required to land the aircraft safely after such event. The annex VII of the European regulation 965/2012 [11] specifies in its paragraph NCO.OP.125 operational reserves which are mandatory for normal flight operations. The required reserve depends on the type of flight operation: reserves for flights according to "Visual Flight Rules" (VFR) differ from flights using "Instrument Flight Rules" (IFR). For VFR-flights in the vicinity of an airfield, it is required to provide reserve energy for a traffic pattern with a flight time of 10 minutes. Although this flight time is intended as a normal flight reserve, it could be a suitable value for the required flight time after a failure of a combustion engine to safely land the aircraft by a normally skilled pilot. This flight time would consequently determine the required battery capacity.

For hybrid-electric aircraft which are propelled by multiple propellers according to CS-23 / CS-25 similar considerations can be carried out, considering the specific paragraphs e.g. CS 23.2120 and CS 25.121 for the propulsion components which generate propulsive power and for the components which provide electric power e.g. battery systems, fuel cells and generator systems.

4. ENERGY RESERVES DURING CRUISE FLIGHT

A failure of a combustion engine in a conventional multi-engine aircraft is associated with a loss of propulsive power. As the remaining combustion engine(s) is/are sized to CS-23 or CS-25 to provide power for a climb flight, the aircraft can continue its cruise flight – in some case with a reduced flight altitude. Furthermore, the stored fuel provides sufficient energy to reach an airport for an emergency landing. This however is not always the case for hybrid-electric aircraft as described in the introduction. If only one combustion engine is installed, the energy stored in the on-board fuel cannot be used for the remaining flight. Hybrid-electric propulsion systems, which are equipped with two combustion engines might convert only a fraction of the energy required for the remaining flight after a failure of one combustion engine from the fuel. This can be the case if combustion engines are applied, which are downsized to cruise power for an increased thermal efficiency. Similarly, if the combustion engines are positioned at the wing tips as intended by the hybrid-electric PEGASUS concept [6], additional electric power is required to compensate the yawing moment of the remaining gas turbine and provide flight time to reach a suitable diversion airport for an emergency landing.

Generalized data for the distance to such a diversion airport is not available and an educated assumption is non-trivial. The National Business Aviation Association (NBAA) provides in its range format [12] an assumption for the distance from a destination airfield to an alternate airfield. This range is part of the required reserve for flights according to Instrument Flight Rules and is assumed to be 100 nautical miles for turbo-prop driven business aircraft and 200 nautical miles for jet business aircraft. However, the intent of the range format was to "provide a standard for prospective aircraft purchasers to use in comparing the performance of various aircraft". It does not state a general existence of an alternate airport within the stated ranges.

The required range of a hybrid-electric aircraft after a failure of a combustion engine or a battery pack is a design parameter which affects the performance of the aircraft. If the range is longer than required, the mass and consequently, the energy demand of the aircraft will be increased. If the range is below a practical value, the operation of the aircraft would be limited. As a result, a more detailed analysis is needed to determine the required value of this design parameter. The analysis is carried out for Europe and the continental part of the United States of America, which is a key market for general aviation aircraft. According to the General Aviation Manufacturers Association [13] 62 % of piston-driven airplanes manufactured worldwide were sold to North America in 2018 – 11 % were sold to Europe.

4.1. Diversion airports

For the determination of the required range of a hybrid-electric aircraft after a failure of one propulsion component, the position data of suitable diversion airports in the investigated region is needed. The Aeronautical Information Publication (AIP) with its chapter Aerodromes (AD) contains all relevant information of airports and airfields, which are necessary for pilots to plan and conduct flights. It contains e.g. latitude, longitude and elevation of the airfield, length and width of runways as well as radio frequencies and further operational data. In [14] an electronic version of the AIP data is available, which was converted to a MATLAB-compatible format and used for the further investigation. The data base comprises of e.g. 20,671 civil airfields for the United States of America. Filtering out heliports, closed airfields, seaplane bases and airfields without a specification of the runway surface leaves 13,283 airfields for consideration. For the investigated part of Europe, the AIP was obtained for the 27 member states of the European Union as well as the United Kingdom, Norway, Switzerland, the Balkans, Ukraine and Belarus. Filtering out heliports, military and closed airfields as well as mountain airfields on glaciers and seaplane bases left 3,808 airports for the investigation.

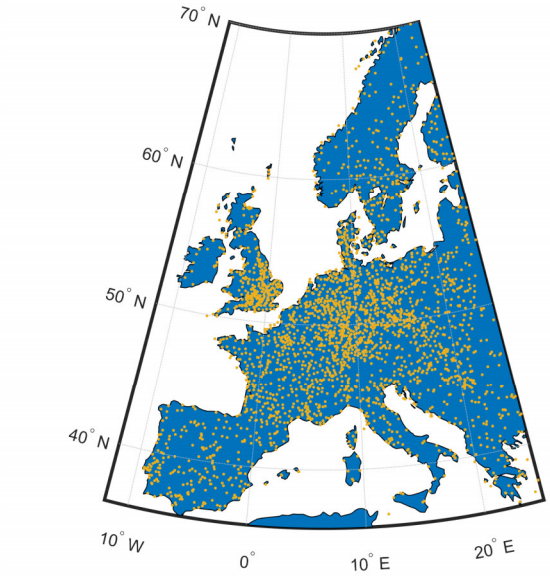

FIG. 4: Location of airports with a runway length greater than 650 m in Europe

The data of the airfields is filtered further for different runway lengths and specific types of runway surface. As a result, data sets are obtained containing all airports with a runway length greater than a specific value. The required runway lengths and surfaces are summarized in TAB. 2 and can be related to an exemplary aircraft representing a specific aircraft class.

Runway length	Surface of runway	Exemplary aircraft
650 m	Asphalt, concrete, grass or gravel	Diamond DA-40, Pilatus PC-12
850 m	Asphalt or concrete	Beech 1900D
1000 m	Asphalt or concrete	ATR-72-600
1150 m	Asphalt or concrete	ATR-42-600
1500 m	Asphalt or concrete	Airbus A320

TAB. 2: Landing field lengths and required surface of different aircraft

In FIG. 5 the influence of the runway length on the number of airports in the USA is shown. The number of airports is significantly reduced for increased runways lengths.

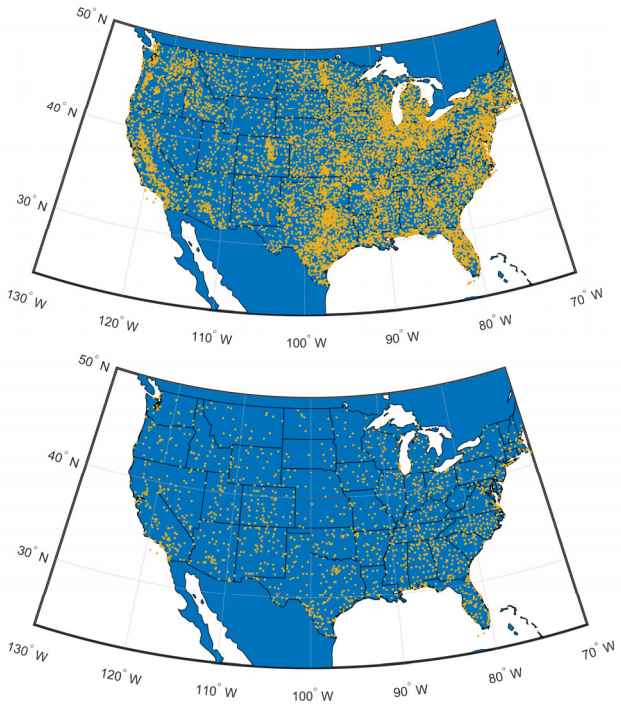

FIG. 5: Location of airports with a runway length greater than 650 m (above) and greater than 1,500 m (below) in the investigated part of the USA

4.2. Aircraft positions

As a next step, a mesh of possible aircraft positions over land was created expressed in latitude ϕ and longitude λ. Aircraft positions over sea and islands, except Great Britain and Ireland, were excluded at this stage. The mesh applied in the calculation consists of positions with a spacing of 1/60° in latitude $\Delta\phi$ and longitude $\Delta\lambda$, which corresponds to a spacing of approximately 1 nautical mile. In FIG. 6 an exemplary mesh is shown with a spacing of 1° in latitude and longitude. In Europe the mesh was created for latitudes from 36°N to 70°N and for longitudes from 12°W to 25°E.

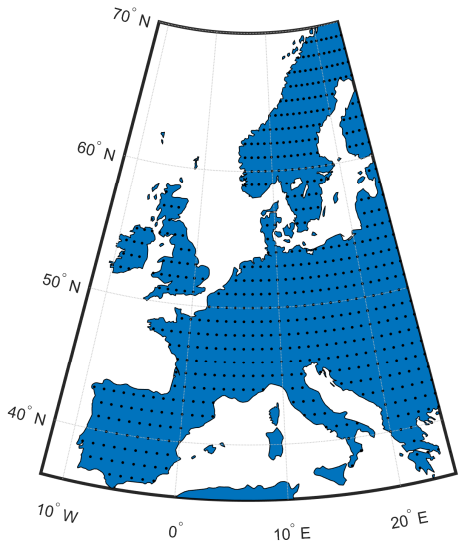

FIG. 6: Exemplary visualization of investigated aircraft positions in Europe with a spacing of 1° in latitude and longitude – the calculation was carried out with a spacing of 1/60°, which results in a spacing of approximately 1 nautical mile

Consequently, the shortest distance of each aircraft position to the suitable diversion airports is determined, by calculating the length of the great circle R to each individual airfield using the following equation, where C_{Earth} denotes the circumference of the Earth and ζ describes the angle of the great circle, and determining the minimum value R_{min}.

$$R = \zeta \cdot C_{Earth} \tag{6}$$

The angle ζ can be calculated by the following equation [15], where ϕ_A and λ_A describe latitude and longitude of the aircraft position and ϕ_B and λ_B denote the coordinates of the airport. The closest airport is then determined for each investigated aircraft position.

$$\cos\zeta = \sin\phi_A \cdot \sin\phi_B + \cos\phi_A \cdot \cos\phi_B \cdot \cos(\lambda_A - \lambda_B) \tag{7}$$

The results of the calculation are shown in the histograms in FIG. 7. The results are categorized in bins where each bin covers a certain spectrum of distances. E.g. the first bin contains all distances from zero to five kilometers. By plotting the number of values contained in each bin, an estimate of the probability distribution of the continuous variable can be shown.

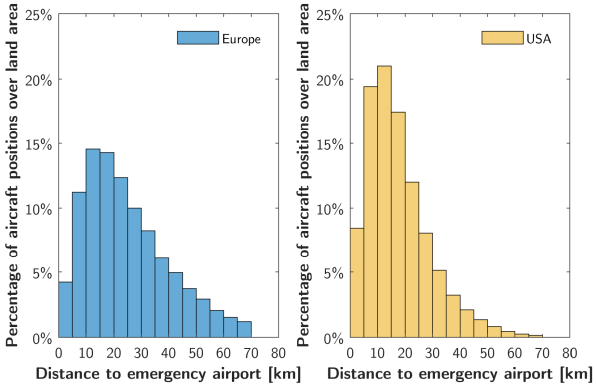

FIG. 7: Results of calculation to determine nearest suitable airport for emergency landing

A cumulative frequency analysis can be performed, where it is determined how often, in other words, with which frequency, the distance to the nearest diversion airport is below a certain value. For the calculation of the cumulative frequency the results need to be sorted from the lowest to the highest value. Consequently, the cumulative frequency $F(x)$ can be calculated using the following equation, where n corresponds to the total number of data points and $M(x)$ is the number of data points below the threshold x. In FIG. 8 the resulting curve is plotted for the USA and Europe. It can be deduced that for 95 % of the aircraft positions in the USA a suitable diversion airport with a runway of at least 650 m exists within a distance of 44 km. For 99 % of the aircraft positions this distance increases to 63 km. For the investigated part of Europe, 95 % and 99 % of the aircraft positions possess a distance to a suitable airfield of less than 67 km and 90 km respectively. For a plausibility check, the mean airport density of the USA is compared to the mean airport density of Europe, which reveals that in the USA 0.95 airports with a runway of 650 m or longer exist per 1,000 km^2 whereas in the investigated part of Europe only 0.48 airports exist per 1,000 km^2.

$$F(x) = \frac{M(x)}{n} \tag{8}$$

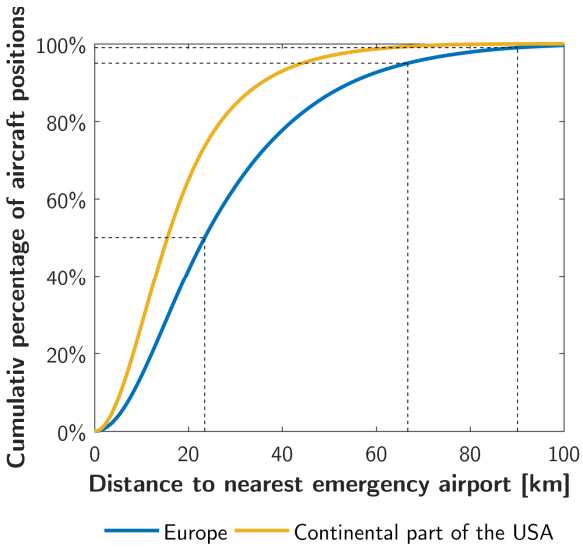

FIG. 8: Plot of cumulative frequency showing e.g. that for 95 % of aircraft positions in Europe a suitable airport with a runway of at least 650 m is within a distance of approx. 62 km

The maximum error of the calculation is evaluated by considering the distance of a possible aircraft position, which is located exactly in between the mesh of aircraft positions. The distance of the great circle between different longitudes is highest at the equator and decreases to South and North Poles. As a result, the maximum error of the calculation is evaluated at the position which is closest to the equator, which is the southern coast of Florida with a latitude of 25°. As the spacing of the positions in latitude and longitude is 1/60°, the maximum error of the calculation can be determined to be 1.26 km.

4.3. Results

For the aircraft designer the 95th percentile will be probably of most importance, as it is a suitable compromise between the possibility to operate the aircraft on the majority of routes and the additional aircraft mass due to the required energy reserve. FIG. 9 compares the results of the 95th percentile for different runway lengths and runway surfaces in Europe and the USA. It can be seen that the USA possesses a denser network of airports as the distance to a suitable diversion airport is lower than in Europe. Furthermore, it can be seen in FIG. 9 how the distance to a suitable diversion airport rises as the required runway length is increased, which is the result of the fewer number of airports with long runways.

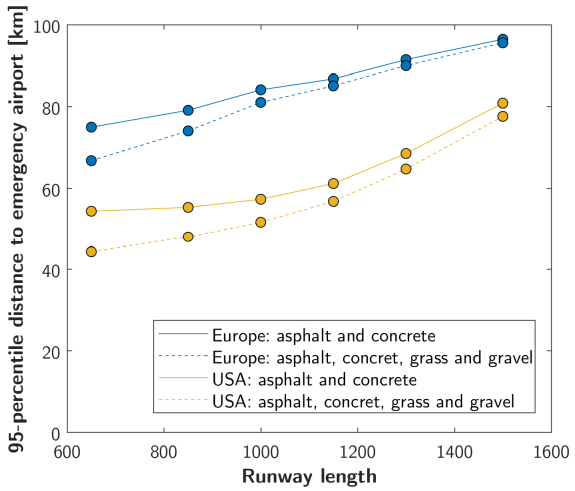

FIG. 9: Comparison of 95th percentile distance to diversion airport for the investigated parts of Europe and the USA depending on required runway length and runway surface

In TAB. 3 the numerical values for the median, the 95th percentile, 99th percentile and the maximum values for the distance to a diversion airport in Europe are given as a reference. The maximum value for the runway length of 650 m corresponds to the position 67.22°N and 18.02°E in the Swedish part of Lapland, where the closest suitable airport is Kalixfors airport (ICAO-code: ESUK), which is situated 129.7 km away.

Runway length	Median	95th percentile	99th percentile	Max.
650 m*	23.5 km	66.8 km	90.1 km	129.7 km
850 m	33.6 km	79.1 km	104.6 km	139.1 km
1000 m	35.9 km	84.1 km	110.6 km	156.3 km
1150 m	37.8 km	86.8 km	113.3 km	159.0 km
1300 m	40.4 km	91.4 km	121.2 km	174.3 km
1500 m	43.5 km	96.4 km	126.9 km	177.9 km

TAB. 3: Distance to a suitable diversion airport for investigated aircraft positions in Europe (=including grass and gravel runways)*

In TAB. 4 the numerical values for the median, the 95th percentile, 99th percentile and the maximum values for the USA are given. The maximum value of 124.1 km for airports with a runway length greater than 650 m corresponds to the position 46.73°N and 69.98°W in Maine, located at the border to Canada. Positions with an increased distance to a diversion airport can be found as well within the USA, e.g. at 42.10°N and 108.22°W in the state of Wyoming.

Runway length	Median	95th percentile	99th percentile	Max.
650 m*	15.5 km	44.3 km	63.0 km	124,1 km
850 m	20.9 km	55.3 km	76.4 km	124.1 km
1000 m	22.7 km	57.3 km	77.7 km	142,7 km
1150 m	25.1 km	61.1 km	79.7 km	142.7 km
1300 m	29.2 km	68.5 km	89.4 km	148.7 km
1500 m	33.0 km	80.8 km	107.7 km	179.9 km

TAB. 4: Distance to a suitable diversion airport for investigated aircraft positions in the USA (=including grass and gravel runways)*

Furthermore, a safety margin should be applied in order to derive from the theoretical range of the great circle to a practical range. A safety factor should be applied in order to account for a delay of the appropriate pilot reaction in case of a failure of a propulsion component. In [16] the response time of 29 general aviation pilots to failures of autopilot systems has been tested. It was found that response times for the detection of "slow" failure types can reach the order of magnitude of 100 seconds. This time can give an indication, which safety margin is required to allow for an appropriate pilot response in case of a failure of a combustion engine in a series hybrid-electric aircraft. For an aircraft with a cruise speed of e.g. 220 km/h (120 knots), this equals to a distance of 6.1 km. A further safety factor should consider adverse head wind conditions, which increase the energy required to reach the diversion airport. If e.g. a “moderate breeze” on the Beaufort Scale is taken as the reference value with wind speeds up to 28 km/h, the flight time of an aircraft with a cruise speed of 220 km/h would be increased by ~15 % and consequently the required energy for flight is increased accordingly. When the aircraft has reached the airport, further flight time is necessary to carry out a traffic pattern, which depends onto the type of airport. For a typical general aviation aircraft, the additional flight range can be in the order of magnitude of 5 km. Exemplary, the influence of the additional reserves is evaluated for a general aviation aircraft with a cruise speed of 220 km/h and a required landing field length of 650 m. The 95-percentile of the distance to a diversion airport in the USA is 44.3 km. Adding the described factors, the required flight range would increase to 62.0 km[1]. Depending on the type of aircraft, flight altitude could be used to reduce the energy necessary to reach the suitable diversion airport.

From the presented data, it can be deduced, that the required landing field length and the geographical area of application are design parameters in aircraft design which might influence the required reserves with its associated mass growth. As one consequence, high-lift systems with an increased maximum lift coefficient or lower wing loadings to achieve lower landing field lengths may be more beneficial for the overall aircraft.

[1] 6.1 km + (44.3 km) · 1.15 + 5 km = 62.0 km

5. ENERGY RESERVES AT DESTINATION AIRPORT

In the following section, the distance from a destination airport to an alternate airport with a suitable runway is determined. This value is expected to have an impact on the performance on purely battery powered aircraft. Due to the limited specific energy of current battery cells, the achievable range of these aircraft can be significantly reduced when increased reserves are required for the flight operation. Hence, the objective is to identify a minimal reserve which allows a safe operation, but compromises the usable flight range as little as possible. The same methodology as described in the section before is applied. In FIG. 10 the determined 95th percentile of the distance to an alternate airport is plotted for different runway lengths and different runway surfaces. It can be seen that the distance in the USA is between 16 % to 36 % lower than in Europe for all investigated runway lengths. Further, it can be observed, how the distance is increased as the required runway length rises because less suitable airports are available.

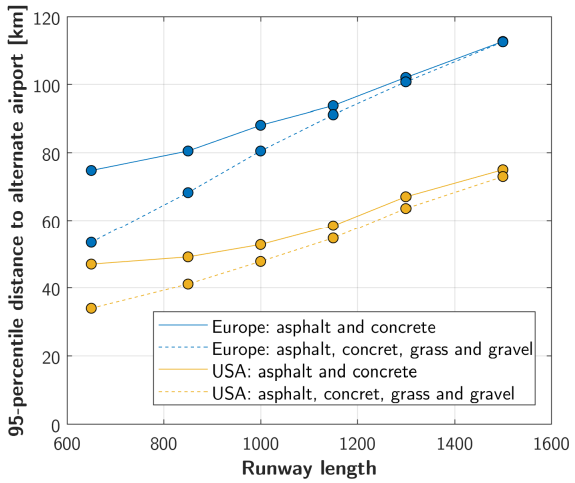

FIG. 10: Comparison of 95th percentile distance to alternate airport for the investigated parts of Europe and the USA

In TAB. 5 the numerical data for Europe is summarized. The maximum value for runway lengths up to 650 m is the distance from Ibiza Airport (ICAO-code: LEIB) in Spain to the alternate airport in Mallorca (ICAO-code: LEPA). The maximum for the runway length of 1500 m corresponds to the airport Sumburgh in Scotland (ICAO code: EGPB) where the suitable alternative is Wick Airport (ICAO code: EGPC).

Runway length	Median	95th percentile	99th percentile	Max.
650 m*	20.0 km	53.3 km	85.6 km	139.5 km
850 m	34.5 km	80.5 km	103.2 km	140.4 km
1000 m	38.2 km	88.0 km	119.9 km	165.8 km
1150 m	41.6 km	93.7 km	125.0 km	165.8 km
1300 m	46.8 km	102.0 km	134.5 km	167.2 km
1500 m	49.1 km	112.6 km	140.4 km	188.5 km

TAB. 5: Distance from a destination airport in Europe to suitable alternative airport (=including grass and gravel runways)*

In TAB. 6 the numerical data for the USA is summarized. The maximum distance within the US for runway lengths up to 650 m is the distance from Grand Marais Cook County Airport, Minnesota, to the suitable alternative Silver Bay Municipal Airport.

Runway length	Median	95th percentile	99th percentile	Max.
650 m*	12.5 km	33.9 km	48.5 km	101.5 km
850 m	23.1 km	49.0 km	68.4 km	124.0 km
1000 m	25.8 km	52.6 km	74.0 km	124.0 km
1150 m	27.4 km	58.3 km	80.2 km	124.0 km
1300 m	30.6 km	67.0 km	91.7 km	124.0 km
1500 m	32.6 km	74.9 km	104.5 km	171.4 km

TAB. 6: Distance from a destination airport in the USA to suitable alternative airport (=including grass and gravel runways)*

If airports would be evenly distributed in Europe and the USA, the distance from the considered aircraft positions to a diversion airport, investigated in the section before, should be lower than the distance from a destination airport to an alternate airport. If the airports however would be clustered, leaving large areas without any airports, then the distance from the investigated aircraft position to a diversion airport should be greater than the distance from a destination airport to a suitable alternate airport. Comparing the data for Europe in FIG. 9 and FIG. 10 indicates that a slight clustering of airports occurs in Europe and the USA.

6. CONCLUSION

A propulsion component failure of a series hybrid-electric aircraft during take-off was investigated. It was shown that with the segmentation of the battery system into a specific number of battery packs, a hybrid-electric propulsion system can be designed which can handle the failure of a combustion engine as well as the failure of a battery pack.

Further, the required flight range of a hybrid-electric aircraft after a failure of a propulsion component during cruise flight was determined. The aim was to identify the minimum additional flight range, which enables a safe operation in the significant majority of Europe and the USA, but at the same time influences the performance of the aircraft as little as possible. Therefore, the data of airports in Europe and the USA was obtained from an electronic version of an Aeronautical Information Publication (AIP). The data was categorized for different minimum runway lengths, which correspond to different types of aircraft. A mesh of aircraft position in Europe and the USA was created and consequently, the distance for each position to the nearest, suitable diversion airport was determined. With a cumulative frequency plot, the 95th percentile of this distance to the nearest diversion airport was determined. It could be shown that in the USA this required flight range is lower for all runway lengths. Exemplary, the 95th percentile of the distance to the nearest diversion airport with a runway length greater than 650 m of any aircraft position in the USA was 44.3 km whereas in Europe the same value increased to 66.8 km. As the determined distances were plain great circle distances, necessary safety margins were discussed covering human factors, adverse wind conditions and a traffic pattern at the diversion airport.

The same methodology was applied in order to determine the distance from a destination airport to an alternate airport

with a suitable runway length. The objective was to identify a minimum distance which allows a safe operation but does not decrease the flight range for normal operation. Due to the limited specific energy of current battery cells, purely battery powered aircraft would specifically benefit from a low distance to an alternate airport. Again, the 95th percentile of the distance in the USA was lower than in Europe – for all investigated runway lengths. Exemplary, for airports with a runway length greater than 650 m the distance was in the USA 33.9 km and in Europe 53.3 km. The presented data showed, how the distance to an alternate airport is increased as the required runway length rises because less suitable airports are available. This indicates the impact of a landing field length of an aircraft to the corresponding, required operational flight reserves.

7. REFERENCES

[1] D. P. Raymer, Aircraft Design: A Conceptual Approach - Fifth Edition, Reston, Virginia: American Institute of Aeronautics and Astronautics, 2012.

[2] T. C. A. Stokkermans, S. Nootebos and L. L. M. Veldhuis, “Analysis and Design of a Small-ScaleWingtip-Mounted Pusher Propeller,” in *AIAA Aviation 2019 Forum*, Dallas, Texas, 2019.

[3] N. K. Borer, M. D. Patterson, J. K. Viken, M. D. Moore, S. Clarke, M. E. Redifer, R. J. Christie, A. M. Stoll, A. Dubois, J. Bevirt, A. R. Gibson, T. J. Foster and P. G. Osterkamp, “Design and Performance of the NASA SCEPTOR Distributed Electric Propulsion Flight Demonstrator,” in *AIAA Aviation Technology, Integration, and Operations Conference*, Washington, D. C., 2016.

[4] I. Geiß and R. Voit-Nitschmann, “Sizing of fuel-based energy systems for electric aircraft,” *Journal of Aerospace Engineering,* pp. 2295-2304, 2017.

[5] I. Geiß, S. Notter, A. Strohmayer and W. Fichter, “Optimized Operation Strategies for Serial Hybrid-Electric Aircraft,” in *AIAA Aviation Technology, Integration, and Operations Conference*, Atlanta, 2018.

[6] K. R. Antcliff and F. M. Capristan, “Conceptual Design of the Parallel Electric-Gas Architecture with Synergistic Utilization Scheme (PEGASUS) Concept,” in *American Institute of Aeronautics and Astronautics*, Denver, Colorado, 2017.

[7] European Union Aviation Safety Agency, “Special Condition E-19 Electric / Hybrid Propulsion System,” Cologne, 2020.

[8] A. Strohmayer and I. Geiß, “Eco4 a New Generation Hybrid-electric Four Place Aircraft,” in *E2-Flight Symposium*, Stuttgart, 06.10.2017.

[9] M. Voskuijl, J. van Bogaert and A. G. Rao, “Analysis and design of hybrid electric regional turboprop aircraft,” *CEAS Aeronautical Journal,* pp. 15-25, 2018.

[10] F. D. Finger, C. Braun and C. Bil, “Impact of Battery Performance on the Initial Sizing of Hybrid-Electric General Aviation Aircraft,” *Journal of Aerospace Engineering,* 2020.

[11] European Commission, “Commission Regulation (EU) No 965/2012,” Brussels, 2012.

[12] National Business Aviation Association, “NBAA Management Guide,” Washington D.C., 2011.

[13] General Aviation Manufacturers Association, “2018 Annual Report,” Washington, D.C., 2018.

[14] “openAIP - Worldwide aviation database,” 24 08 2020. [Online]. Available: http://openaip.net/.

[15] I. Agricola and T. Friedrich, Elementargeometrie, Wiesbaden: Springer Spektrum, 2015.

[16] D. B. Beringer, “Automation in General Aviation: Responses of Pilots to Autopilot and Pitch Trim Malfunctions,” *Proceedings of the Human Factors and Ergonomics Society 40th Annual Meeting,* 1996.